Professor O. Hittmair and to Professor P. Weinzierl for their encouraging interest. They are also indebted to Dr. E. M. Hörl for carefully reading the manuscript.

[1]S. Y. Tong and A. A. Maradudin, Phys. Rev. 181, 1318 (1969).
[2]R. E. Allen, G. P. Alldredge, and F. W. DeWette, Phys. Rev. Letters 23, 1285 (1969).
[3]R. E. Allen, G. P. Alldredge, and F. W. DeWette, Phys. Rev. Letters 24, 301 (1970).
[4]L. Dobrzynski and D. L. Mills, J. Phys. Chem. Solids 30, 1043 (1969).
[5]L. Dobrzynski, Surf. Sci. 20, 99 (1970).
[6]J. M. Morabito, Jr., R. F. Steiger, and G. A. Somorjai, Phys. Rev. 179, 638 (1969).
[7]S. W. Musser, J. Phys. Chem. Solids (to be published).
[8]J. DeLaunay, Solid State Phys. 2, 219 (1956).
[9]B. J. Birgeneau, J. Cordes, G. Dolling, and A. B. D. Woods, Phys. Rev. 136, A1359 (1964).
[10]W. A. Kamitakahara and B. N. Brockhouse, Phys. Letters 29A, 639 (1969).
[11]W. Drexel, Autumn Meeting of the Austrian and German Physical Societies, Salzburg, Austria, 1969 (unpublished).
[12]W. Ludwig and B. Lengeler, Solid State Commun. 2, 83 (1964).
[13]Owing to symmetry, the conditions of rotational invariance are automatically fulfilled in an infinite cubic crystal.
[14]B. C. Clark, D. C. Gazis, and R. F. Wallis, Phys. Rev. 134, A1486 (1964).
[15]D. C. Gazis and R. F. Wallis, Surf. Sci. 5, 482 (1966).
[16]A. A. Maradudin, Rept. Progr. Phys. 18, 331 (1965).
[17]For our crystal model the essential quantities appearing in Sec. III are given in Ref. 7 as functions of the coupling constants.
[18]T. E. Feuchtwang, Phys. Rev. 155, 715 (1967).
[19]The lattice constant a appears in Eq. (14), as in the scale used for $k_{\parallel}$ the Brillouin-zone boundary $\bar{M}$ corresponds to $k_{\parallel}=\pi$.
[20]D. C. Gazis, R. Herman, and R. F. Wallis, Phys. Rev. 119, 533 (1960).
[21]T. C. Lim and G. W. Farnell, J. Appl. Phys. 39, 4319 (1968).

PHYSICAL REVIEW B VOLUME 2, NUMBER 8 15 OCTOBER 1970

Echo Expansion in the Theory of Alloys*

Richard M. More and Klaus Hacker†
Department of Physics, University of Pittsburgh, Pittsburgh, Pennsylvania 15213
(Received 1 May 1970)

We have obtained a systematic expansion for the trace of the Green's function of electrons moving in a disordered alloy. In our expansion, the terms are classified by a path length which, for some models, takes on discrete values. The expansion is strongly convergent for large complex energies, but seems to be surprisingly useful even for nearly real energies. We present numerical calculations of the density of states for a one-dimensional system.

I. INTRODUCTION

Imagine emitting a pulse of sound from a point into some inhomogeneous environment and then waiting a short time t for the echoes. The result may be calculated *exactly*, knowing the properties of the environment within an influence sphere of radius $\frac{1}{2}ct$ about the initial point, where c is an appropriate sound velocity. We contrast this soluble problem with the very difficult one of reliably calculating the exact sonic dispersion relation in an inhomogeneous medium.

A qualitatively similar situation occurs for electrons in a disordered (or partially disordered) alloy. Of course, there is no strict limit on the velocity of motion of an electron (in a nonrelativistic theory). Nevertheless, over short time intervals, the motion is still essentially confined within an influence sphere, and this suggest the possibility of making a *local* calculation of some aspect of the electron dynamics. In this paper, we explore this possibility. The results are quite simple and interesting.

First, we have obtained a perfectly systematic and convergent "echo" expansion of the trace of the electron Green's function for complex energy z:

$$\mathrm{Tr}G(z)=\sum_L f_L(z)\,e^{ikL}, \quad k\equiv\sqrt{z}\ . \tag{1.1}$$

We consider noninteracting electrons moving in the presence of many "atomic" potentials V_n, with kinetic energy $H_0=p^2/2m$. In the present paper, we limit ourselves to one-dimensional problems with δ-function potentials on the sites of a fixed lattice. None of these limitations are essential in the present method. We define the Green's func-

tion $G(z)$ by the formal equation

$$G(z) \equiv 1/(z - H), \quad H = H_0 + \sum_n V_n . \tag{1.2}$$

The quantity z is the complex energy, and we choose the square root which makes the exponentials in (1.1) decrease as z increases. The successive terms of the expansion (1.1) are labeled by a path length L which indicates their rate of exponential decrease. For substitutional alloys, the possible path lengths L which occur in (1.1) form a discrete set. The functions $f_L(z)$ are algebraic functions of z for sufficiently large z.

Second, the systematic expansion (1.1) is simply a rearrangement of the usual multiple-scattering series,[1-3] i.e., the usual expansion of $G(z)$ in terms of an unperturbed Green's function $G_0(z)$,

$$G_0(z) \equiv 1/(z - H_0) ,$$
$$G = G_0 + \sum_n G_0 T_n G_0 + \sum_n \sum_{m(\neq n)} G_0 T_n G_0 T_m G_0 + \cdots , \tag{1.3}$$

where $T_n(z)$ is the T matrix for the nth atomic potential, defined as the solution of the formal equation

$$T_n(z) = V_n + V_n G_0(z) T_n(z) . \tag{1.4}$$

The exponential factors $\exp(iL\sqrt{z})$ in the expansion (1.1) come from the unperturbed Green's functions in (1.3). Graphically, each $f_L(z)$ arises from closed-loop diagrams in which the total elapsed distance is L and in which various stops at potentials V_n occur. Geometrically, these paths are precisely those giving echoes at the time L/c for the analogous sound-propagation problem. Rearranging the series (1.3) into the echo series (1.1) makes certain troublesome subsequences absolutely convergent even for real energies (see Sec. IV).

Third, we are able to clearly exhibit the rather oblique sense in which the Friedel one-impurity theory becomes correct in the low-density limit.[3-5] This question was raised and discussed (in another context) by Anderson.[3]

Fourth, our results suggest a number of practical programs for calculating properties of disordered alloys. We may attempt to calculate $\mathrm{Tr}G(z)$ for complex energies and then analytically continue it back to real energy, thereby obtaining the density of states

$$\rho(E) = -(1/\pi) \lim \mathrm{Im}\, \mathrm{Tr}G(E + i\eta) \quad \text{as } \eta \to 0^+ . \tag{1.5}$$

Alternatively, as has been suggested by Langer,[6] we may compute $\mathrm{Tr}G(E_0 + i\Gamma)$, where the series is convergent. The result directly gives a Lorentzian average (of width Γ) over the nearby real density of states, omitting only the high-frequency variations.

Finally, directly computing the terms $f_L(z)$ for large z, we may compare (and contrast) with the results of approximation techniques of the self-energy type.[3,7-10] Used in this last fashion, the echo expansion is related to a well-known moment-expansion technique.[10] When possible, one expands the trace of a Green's function in the fashion

$$\mathrm{Tr}\frac{1}{z - H} = \frac{1}{z} + \frac{1}{z^2}\mathrm{Tr}H + \frac{1}{z^3}\mathrm{Tr}H^2 + \cdots , \tag{1.6}$$

and thus the limit of $\mathrm{Tr}G(z)$ for large z is related to moments of the total density of states. This expansion (1.6) cannot be used if the spectrum of H is unbounded, as for $H_0 = p^2/2m$; the echo expansion (1.1) is an extension of (1.6) to that case.

Because the echo expansion is an exact treatment and not at all an approximation scheme, there is no restriction to "nearly ordered" or "highly disordered" systems. However, in its present form, the echo expansion is only a practical approach for systems with *lumped* inhomogeneities. The expansion coefficients $f_L(z)$ are easily evaluated if the atomic potentials V_n are placed substitutionally on lattice sites and are geometrically small compared to their separations. The one-dimensional Kronig-Penney-like lattices represent the extreme limit in which these convenience conditions are satisfied. In these systems, the disorder is only in the strengths of the δ-function potentials. Since we make no approximation in the treatment of this disorder, we believe that our technique will provide a standpoint for critical evaluation of approximate techniques for dealing with multiple-scattering series.

II. ECHO EXPANSION

In this section, we give a constructive definition of the echo expansion. While this discussion is not strictly systematic, we think it permits the clearest and most rapid exposition. Our approach will be to show that terms of the type shown in Eq. (1.1) emerge from evaluation of the traces of the various terms in the multiple-scattering series (1.3). When the reader understands the method of grouping the multiple-scattering terms, we think that it will be obvious that the grouping is indeed perfectly systematic and complete (i.e., each multiple-scattering term enters into one echo-series term). The conclusive check, however, will be the application of the series to the soluble Kronig-Penney model, considered in Sec. III.

In the present section, we give formulas appropriate to the disordered one-dimensional δ-function potential problem, defined by the potential

$$v(x) = \sum_n \lambda_n \delta(x - nb) \tag{2.1}$$

appearing in a Schrödinger equation

$$-\psi'' + v(x)\psi = k^2\psi(x) \ .$$

The constant b in (2.1) is the lattice spacing, and the coefficient λ_n gives the strength of the "atomic" potential on the nth site. We simulate a two-component substitutional alloy if we allow the λ_n to take on two values. Many of our formulas and statements about general analytic properties must be slightly modified if the potentials do not have the simple form (2.1), and so we restrict ourselves to this class of potentials for the duration of this paper.

The total potential (2.1) may then be regarded as a superposition of local potentials $v_n(x)$ of the form

$$v_n(x) = \lambda_n \delta(x-a) \ . \tag{2.2}$$

Using the one-dimensional unperturbed Green's function in the space-energy representation,

$$G_0(x, x'; z) = (1/2ik)\, e^{ik|x-x'|}, \quad k \equiv \sqrt{z} \tag{2.3}$$

we easily solve Eq. (1.4) for the T matrices:

$$T_n(x, x'; z) = \frac{\lambda_n}{1-\lambda_n/2ik}\, \delta(x-a)\, \delta(x'-a) \ . \tag{2.4}$$

For convenience in the sequel, we define the numerical constant

$$t_n \equiv \lambda_n/(2ik - \lambda_n) \ . \tag{2.5}$$

Now, we are equipped to begin consideration of the traces of the terms of the multiple-scattering series (1.3).

In order to obtain finite results, we wish to consider the traces per unit volume of alloy, i.e.,

$$\mathrm{Tr}G(z) \equiv \lim \frac{1}{L} \int_0^L G(x, x; z)\, dx \quad \text{as } L \to \infty. \tag{2.6}$$

In the sequel, this will be the usage of the symbol "Tr" with the capitalized T. The symbol "tr" will stand for the trace *without* the division by L and, of course, will only be applied to bounded operators.

As an example of definition (2.6), consider the contribution of the unperturbed Green's function G_0. The result is clearly

$$\mathrm{Tr}G_0(z) = 1/2ik \ .$$

This is the first trace encountered in examining the multiple-scattering series.

The next class of traces correspond to the one-atom terms

$$\sum_n \mathrm{Tr}(G_0 T_n G_0) \ .$$

We assume that there is no large-scale order in the atomic compositions. That is, the *a priori* probability that site n carries potential λ_n is assumed to be independent of n. This assumption does *not* preclude any type of *correlation* among the alloy components. We make no assumption on the pair correlation function, but, rather, assume that the one-atom distribution function is independent of position. In a perfectly ordered *ABABAB...* alloy, this amounts to averaging over two configurations shifted by one lattice spacing (and each having identical density of states).

With this assumption, and recognition that there are L/b sites in length L, we have

$$\sum_n \mathrm{Tr}(G_0 T_n G_0) = (1/b)\, \mathrm{tr}(G_0 T_1 G_0) \ ,$$

where the right-hand expression must, of course, be appropriately averaged over values of λ_1.

Then we assert that the first term in the "echo expansion" of (1.1) is the sum of the two above quantities,

$$f_0(z) = \mathrm{Tr}G_0 + (1/b)\, \mathrm{tr}(G_0 T_1 G_0) \ . \tag{2.7}$$

These terms (as we show below) are all the contributions to $\mathrm{Tr}G(z)$ which do not decrease exponentially for large complex energy.

We further evaluate the one-atom terms by recognizing two quite general equations (applicable also to three-dimensional problems),

$$-\frac{d}{dz} G_0 = G_0^2 \quad , \tag{2.8a}$$

$$-\frac{d}{dz} T_n = T_n G_0^2 T_n \ . \tag{2.8b}$$

Using the second of these equations, we see

$$\mathrm{Tr}G_0^2 T_n = -\frac{d}{dz}\, \mathrm{tr}\, \ln T_n \ .$$

From this expression, we can immediately read off the Friedel formula for the change in density of states of a one-impurity system. The imaginary part of the natural logarithm of T_n is, for real energies, the usual phase shift. In three dimensions, this leads to the formula

$$\delta\rho^{(1)}(E) = \frac{2}{\pi} \sum_{l=0}^{\infty} (2l+1) \frac{d}{dE}\, \delta_l(E)$$

for the one-atom contribution to the change in density of states. We can see that these Friedel terms dominate at large complex energy.

For our model one-dimensional problem, Eq. (2.7) is evaluated to be

$$f_0(z) = \frac{1}{2ik} - \frac{1}{b} \frac{d}{dz} \ln(2ik\, t_1) \ . \tag{2.9}$$

Here again, an average over the occupations of site 1 is implied, i.e., over the possible values of t_1.

Now we consider the largest of the exponentially decreasing terms of (1.1). These correspond to the shortest permitted echo path, which has length $L = 2b$. The result is

$$f_{2b}(z)\, e^{2ikb} = -\frac{1}{b}\,\frac{d}{dz}\,\mathrm{tr}(G_0T_1G_0T_2)\,. \qquad (2.10)$$

The relation to the terms of the multiple-scattering series is clarified by performing the indicated differentiations in (2.10) using formulas (2.8). We see

$$-\frac{d}{dz}\,\mathrm{tr}(G_0T_1G_0T_2) = \mathrm{tr}(G_0T_1G_0T_2G_0 + G_0T_2G_0T_1G_0$$

$$+ G_0T_1G_0T_2G_0T_1G_0 + G_0T_2G_0T_1G_0T_2G_0)\,, \qquad (2.11)$$

and the resulting quantities are indeed traces of terms in the multiple-scattering series. Notice the unequal powers of T_n appear. That is, the contributions to $f_{2b}(z)$, a typical echo term, are not homogeneous in powers of T_n. Instead, as we have remarked, the terms are grouped by their rate of exponential decrease for large complex z and *this* feature is the basis of our rearrangement of the multiple-scattering series.

The detailed question of correct counting of contributions such as (2.10) is settled more conclusively in Sec. III. For now, notice that because we want the trace per distance b, we may limit ourselves to contributions associated with a typical unit cell. Then, while the value of T_1 is averaged over, the values of T_2 are fixed by appropriate conditional probabilities.

The general contribution having an exponential decrease rate determined by $L = 2b$ is associated with a trace involving two adjacent "atoms." We have made the *convention* of associating each such contribution with the atom on the left. Thus, the trace

$$-\frac{1}{b}\frac{d}{dz}\,\mathrm{tr}(G_0T_0G_0T_1)$$

is also counted, but associated with the unit cell of T_0.

We represent the trace of Eq. (2.10) by the diagram of Fig. 1. The circles represent T matrices and the lines represent factors G_0. This is a diagram in configuration (position) space, and the "path length" L is simply the circumference of the diagram.

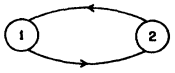

FIG. 1. Diagram corresponding to echo path length $L = 2b$. The circles represent atomic T matrices, and they are joined by unperturbed Green's functions.

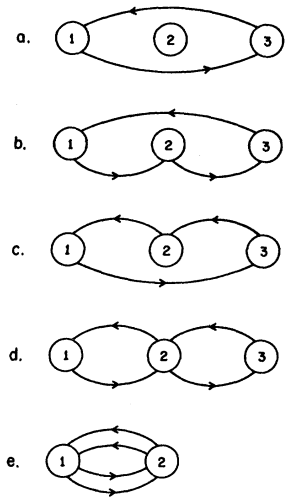

FIG. 2. Diagrams corresponding to path length $L = 4b$.

For the one-dimensional model under consideration, the value of (2.10) is given by

$$f_{2b}(z)\, e^{2ikb} = -\frac{1}{b}\,\frac{d}{dz}\,(t_1t_2\, e^{2ikb})\,, \qquad (2.12)$$

in which the quantities t_1 t_2 must be appropriately averaged taking the correlations into account.

The next set of terms correspond to path length $L = 4b$. We indicate them graphically in Fig. 2. The contribution to the trace of $G(z)$ of graph (a) of Fig. 2 is equal to

$$-\frac{1}{b}\,\frac{d}{dz}\,\mathrm{tr}(G_0T_1G_0T_3)\,,$$

and the total contribution of graphs (a)–(d) is given in the more convenient expression

$$-\frac{1}{b}\,\frac{d}{dz}\,\mathrm{tr}[G_0T_1(1+G_0T_2)G_0T_3(1+G_0T_2)]\,. \qquad (2.13)$$

Graph (e) of Fig. 2 contributes

$$-\frac{1}{2}\,\frac{1}{b}\,\frac{d}{dz}\,\mathrm{tr}(G_0T_1G_0T_2G_0T_1G_0T_2)\,. \qquad (2.14)$$

Evaluating these formulas for the one-dimensional model, we obtain

$$f_{4b}\, e^{4ikb} = -\frac{1}{b}\,\frac{d}{dz}\,\{e^{4ikb}[t_1(1+t_2)^2\, t_3 + \tfrac{1}{2}\, t_1^2 t_2^2]\}\,. \qquad (2.15)$$

The terms contributing to $f_{4b}(z)$ contain (again) various powers of the T_n, ranging from $O(t^2)$ to $O(t^5)$. As we commented before, the common fea-

ture of these terms is the circumference of the space path representing them. In distinguishing contributions (2.13) and (2.14), we see the beginnings of a significant qualitative differentiation of the echo paths: those which [as in (2.13)] reach out to the boundary of the influence sphere and those [as in (2.14) above] which are highly folded and remain primarily near the center.

In the expression (2.14), there is a numerical factor $\frac{1}{2}$ which is needed to restore correct counting. This is necessary because of the differentiation technique which we employ.

In these terms, we have associated the contribution of each graph with the leftmost "atom" touched. This convention assures proper counting in general. The contribution of graph (a) of Fig. 2 is, of course, precisely the analog of the contribution of Fig. 1.

The terms corresponding to the next possible path length ($L = 6b$) are generally similar, although more numerous. Here, one must be quite careful not to doubly count diagrams, i.e., to remember that because of the cyclic invariance of the trace, the same contribution may be written in more than one way. The result, evaulated for the one-dimensional δ-function model, is

$$f_{6b}\, e^{6ikb} = -\frac{1}{b}\frac{d}{dz}\{e^{6ikb}[t_1 t_4(1+t_2)^2(1+t_3)^2 + t_1^2 t_2(1+t_2)^2 t_3 + t_1 t_2(1+t_2)^2 t_3^2 + \tfrac{1}{3} t_1^3 t_2^3]\}. \quad (2.16)$$

III. COMPARISON TO SOLUBLE KRONIG-PENNEY MODEL

Consider the Hamiltonian of Sec. II for the special case in which all atomic potentials are the same,

$$H = p^2/2m + \lambda \textstyle\sum_n \delta(x - nb)\ .$$

We then have the usual Kronig-Penney model, for which an exact solution is available.[11] In this section we indicate the comparison with the "echo expansion."

The electron-dispersion relation in the Kronig-Penney model is implicitly given by the formula

$$\cos qb = \cos kb + (\lambda/2k)\sin kb\ . \quad (3.1)$$

In this equation, q is the wave vector of the Bloch wave which has energy $E_{n,q}$. As above, k is simply the square root of this energy.

The density of states is then given by

$$\rho(E) = \frac{1}{\pi}\frac{dq}{dE} = \frac{1}{2\pi k}\left[\left(1 + \frac{\lambda}{2bk^2} - \frac{\lambda}{2k}\frac{\cos kb}{\sin kb}\right)\Big/ \left(1 - \frac{\lambda^2}{4k^2} - \frac{\lambda}{k}\frac{\cos kb}{\sin kb}\right)^{1/2}\right]. \quad (3.2)$$

The trace of the exact Green's function is now obtained by performing a Cauchy integral involving the density of states (3.2). The result, Eq. (3.3) below, is essentially the same as (3.2). However, the Cauchy integration must be performed very carefully, and we have deferred that calculation to the Appendix. The version given there is more generally applicable to any one-dimensional periodic lattice.

The resulting expression is then

$$\mathrm{Tr}G(z) = \frac{1}{2ik}\left[\left(1 + \frac{\lambda}{2bk^2} - \frac{\lambda}{2k}\frac{\cos kb}{\sin kb}\right)\Big/ \left(1 - \frac{\lambda^2}{4k^2} - \frac{\lambda}{k}\frac{\cos kb}{\sin kb}\right)^{1/2}\right]. \quad (3.3)$$

The branch cuts of the square root are defined in the Appendix.

The formula $\mathrm{Tr}G(z)$ depends upon $k = z^{1/2}$ in two ways: algebraically (i.e., in powers of k) and exponentially, in the form $\exp(\pm ikb)$. As b is positive, the exponential $\exp(ikb)$ is small when the imaginary part of k is positive. What we shall do is to systematically expand $\mathrm{Tr}G(z)$ with respect to this small exponential, without making any expansion in the algebraic k dependence. Thus, for example, we make the expansion

$$\frac{\cos kb}{\sin kb} = -i\left(1 + 2\sum_{n=1}^{\infty} e^{2ikbn}\right). \quad (3.4)$$

The resulting expansion for $\mathrm{Tr}G(z)$ is given by

$$\mathrm{Tr}G(z) = \frac{1}{2ik} + \frac{1}{2k^2 b}\, t + e^{2ikb}\left(\frac{t^2(1+t)}{k^2 b}(1 - ikb) - \frac{t^3}{ik}\right) + \cdots\ . \quad (3.5)$$

It is a simple mathematical exercise to verify that precisely this expansion is given by formulas (2.9), (2.12), (2.15), and (2.16). It is actually easier to compute the terms of the echo series than to expand the exact answer.

From Eq. (3.4), we see that the echo expansion is formally on its circle of convergence (at best) for real energies. For sufficiently large complex energy, it is absolutely convergent.

In Sec. V, we discuss the numerical applicability of the echo series.

IV. GENERAL FEATURES OF THE EXPANSION

At this point we can conveniently survey our results. The basic idea is to regularize the multiple-scattering series [Eq. (1.3)] by computing it for

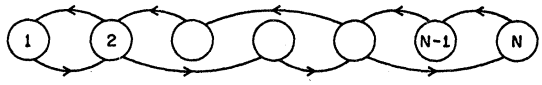

FIG. 3. Typical diagram corresponding to path length $L=2(N-1)b$.

complex energy, where the unperturbed Green's function is exponentially small. This was suggested to us by the coherent-potential approximation of Soven *et al.*[9,10] However, those authors chose a particular complex energy in order to optimize the approximation of $\mathrm{Tr}G_0(E+i\Gamma)$ to $\mathrm{Tr}G(E)$. Instead, we use the imaginary part of the energy as a parameter of no physical significance and attempt to compute the actual terms of the multiple-scattering series.

In a sense, this is a departure from the "mainstream" of work on the multiple-scattering series for disordered alloys. Most of the literature develops self-energy schemes for performing approximate infinite-order summations of the multiple-scattering series.[2,7,8,12] The present work instead explicitly sums a finite number of early terms of the series. The results of this procedure are sometimes very satisfactory (see Sec. V). In other cases, they are quite inadequate, and we will have to alter the method to obtain a series useful for real energies.

The other ingredients of the method are purely technical. The differentiation technique introduced in Sec. II is convenient in evaluation of the traces of the multiple-scattering-series contributions. Furthermore, it automatically groups terms of same path lengths into simpler generating functions, e.g., Eqs. (2.10), (2.13), etc. However, this technique is neither essential nor surprising.[13] It is closely related to "root-point" methods commonly used in statistical mechanics.[6]

The echo expansion does have some advantages. Consider the following subseries of the multiple-scattering series (2.13):

$$\sum_N C'_N, \quad C'_N \equiv -\frac{d}{dz}\,\mathrm{tr}(G_0T_1G_0T_N)\,. \tag{4.1}$$

This subseries would be the first encountered if (1.3) were summed without rearrangement. However, (4.1) is *not* absolutely convergent when evaluated for real energies.

From the viewpoint of the echo expansion, this is only one of a class of contributions exemplified by the diagram of Fig. 3. These diagrams have path length $L=2N-2$ and total elapsed distance $D=L$. The various diagrams of the class differ by having various "optional" stops at the potentials between sites 1 and N. We sum the entire class of contributions in the formula

$$C_N = -\frac{d}{dz}\,\mathrm{tr}[G_0T_1(1+G_0T_2)\cdots(1+G_0T_{N-1}) \times G_0T_N(1+G_0T_{N-1})\cdots(1+G_0T_2)]\,. \tag{4.2}$$

Now let us consider (4.2) for *real* energies. In that case we have

$$t_n = \lambda_n/(2ik-\lambda_n)\,,$$

with real k, so that

$$|1+t_n| \equiv r < 1\,. \tag{4.3}$$

Then, the contribution of the class of diagrams summed in (4.2) is much smaller than the one diagram without the optional stops (i.e., $C_N \ll C'_N$) since

$$C_N \propto r^{2N-2} \propto e^{-\alpha L}, \quad \alpha > 0\,. \tag{4.4}$$

Thus, by summing the diagrams consistently by path length, we obtain an absolute convergence even for real energies. Of course, the class of diagrams counted in (4.2) is not *all* the diagrams of path length L, but only the subclass which reach out all the way to the edge of the influence sphere. There will still be folded paths of length L which make appreciable contributions.

Unfortunately, the exponential convergence of Eq. (4.4) is not yet the interesting exponential convergence associated with the mean free path.[14] The result (4.4) holds even for the ordered Kronig-Penney model, where the true mean free path is infinite. To obtain information about the correct mean free path, we must compare appropriate averages of powers of t_n with powers of averages; this is a difficult question.

Nevertheless, (4.4) suggests that the echo expansion may even be of interest for real energies. This is a very bold conjecture, and indeed there is no general reason to expect the series to be convergent for real energies. For the ordered Kronig-Penney model, as we showed in Sec. III, the series is at best on its circle of convergence for real energy.

We have attempted to apply the echo series to directly compute the density of states of ordered and disordered systems. We give some more details in Sec. V; here we summarize our experience by saying that the series seems to work very well for positive energies.

For the case of attractive δ functions ($\lambda_n < 0$) in which the individual T matrices have a bound-state pole, the series is *not* convergent in the negative-energy range. To be more precise, it cannot be used to directly compute the density of states for real energies, but is only rendered convergent by evaluating it for sufficiently large imaginary part

of the energy.

However, for repulsive potentials ($\lambda_n > 0$) the series behaves much better. The numerical results of Sec. V show that the echo series provides a simple and practical way to compute the density of states in the region of positive energies.

The real question about the usefulness of the method concerns its extension to three-dimensional systems with realistic potentials. We believe that the echo expansion will be quite useful for discussing a restricted class of three-dimensional systems.

Formulas such as (2.10), (2.13), and (2.14) are applicable also in three-dimensional systems, because the basic differentiation formulas (2.8) apply also in three dimensions. The three-dimensional multiple-scattering series then has an echo expansion, but with certain important differences.

First, in three dimensions the number of echo paths is considerably larger. This will provide a practical limitation on applications of this method. Of course, enumeration of the echo paths is a geometrical problem independent of the potentials present at the lattice sites, so that it may be done once for all.

Second, the integrals in the traces, such as (2.10), (2.13), etc., are required. In one extreme case, they may be evaluated without any explicit machine quadrature, and this is the extreme in which the echo expansion will be most useful.

Let a represent the size of the potentials, i.e., their radius. Let R_{ij} represent their separation. Then, the trace $\mathrm{tr}(G_0 T_i G_0 T_j)$ may be expanded in powers of (a/R_{ij}) by making the usual expansion in the unperturbed Green's functions. In that case, i.e., for

$$a/R_{ij} \ll 1 , \tag{4.5}$$

the trace reduces to the on-shell scattering amplitudes, i.e., to the scattering phase shifts.

In this extreme case, the contribution of any diagram is obtained simply by multiplying together factors $G_0(R_{ij})$ and scattering amplitudes with the appropriate angles indicated in the diagram.[15]

Since this extreme model still permits disorder in the strengths of the atomic potentials, it will be interesting and convenient to study.

V. NUMERICAL RESULTS

We now discuss the numerical application of the echo expansion to the one-dimensional problem of Sec. II. While our results are of some interest already, we anticipate that the techniques can be made considerably more sophisticated.

We have evaluted the Lorentz-averaged integrated density of states $\langle N(E)\rangle_\Gamma$ defined by

$$\frac{\pi}{\Gamma}\langle N(E)\rangle_\Gamma = \int \frac{N(E')\,dE'}{(E-E')^2+\Gamma^2} . \tag{5.1}$$

A simple calculation shows that the Lorentz average of the actual density of states is related to the trace of $G(z)$ by the formula[6]

$$\langle \rho(E)\rangle_\Gamma = -(1/\pi)\,\mathrm{Im}\,\mathrm{Tr}G(E+i\Gamma) . \tag{5.2}$$

In this application, our hope was to choose Γ sufficiently large so that the series "is convergent," and still sufficiently small so that the detailed aspects of the density of states are visible. One of the ways in which the calculation might be made more sophisticated is in developing a systematic method for choosing Γ. After two or three trials, we settled on the value $\Gamma = 0.1$. Smaller values resulted in an oscillatory curve $\langle N(E)\rangle_\Gamma$, which is certainly unacceptable.

First, we compare the integrated density of states $\langle N(E)\rangle_\Gamma$ computed by the echo series with exact values (for real energy E). The lattice parameter is chosen to be unity ($b = 1$) and the potential strength $\lambda = 4.0$. In the echo series, we included terms up to $L = 8b$.

The resulting comparison is given in Fig. 4. We see that the values are in very good agreement inside the bands; at the band edge the detailed agreement is not so good. Of course, a finite number of terms of a Fourier series cannot represent a sharp corner well. Despite the departure from the exact density of states at the band edges, we feel that the approximate curve gives a generally good picture of the density of states and the energy gaps.

Next, numerical calculations were performed for the case of a one-dimensional lattice (again with $b = 1$) containing vacancies. By vacancies, we mean lattice sites with no potential ($\lambda = 0$). The "occupied" sites again had $\lambda = 4.0$. We assumed that the vacancies were distributed randomly, so that the probability that any site was vacant did not depend on the environment.

In Fig. 5, we compare the pure lattice with the results for three concentrations of vacancies (10, 20, and 30%). There are several interesting features of these curves.

In the lower half of each band (away from the threshold), we have the behavior predicted by the "rigid-band theorem." The density-of-states curve is shifted to the left without gross distribution, and the shift is roughly proportional to the vacancy concentration. We anticipate that this simple result would not occur if the impurity potential gave rise to scattering with some more dramatic energy dependence.

Next, we think it is quite interesting to contrast the quite different effect of the vacancies on the

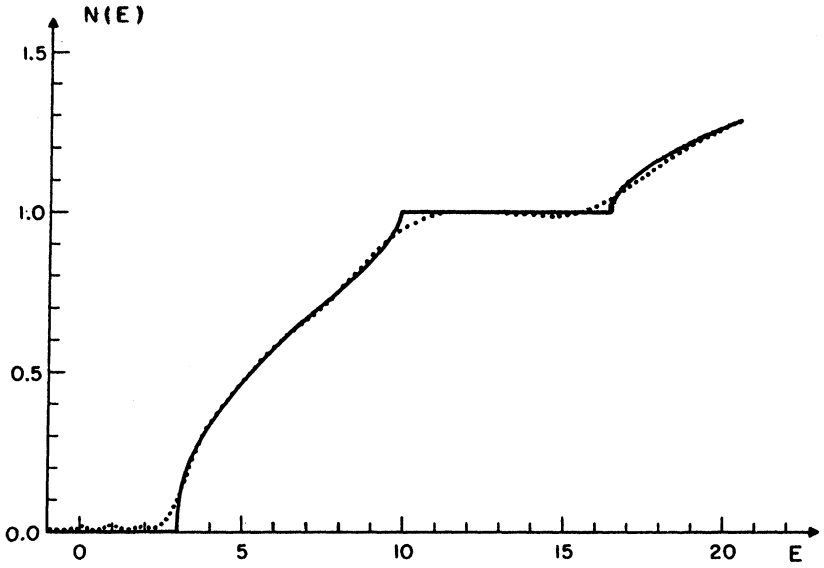

FIG. 4. Comparison of the echo series with the exact-ordered Kronig-Penney model. The solid line represents the exact result for $b = 1$, $\lambda = 4$. The dotted curve was obtained from the echo series including terms with $L = 8b$, with $\Gamma = 0.1$.

two band edges at $E \cong 10$ and $E \cong 15$. The lower band edge is essentially unaffected by the vacancies, whereas the upper band edge is moved to lower energies.

The physical origin of this effect is quite simple. At such a band edge, the electron wave functions are standing waves. At the lower band edge, the standing wave has a node on each atomic site; at the upper band edge, it has a maximum. Then the introduction of vacancies or indeed arbitrary impurities in place of the atoms cannot affect the energy of the states near the lower band edge ($E = 10$), whereas alloying will seriously affect the upper edge.

We think it is quite interesting that this effect emerges from the echo expansion. For while it is easily understood in terms of the wave functions of the pure infinite Kronig-Penney lattice, here we obtain the result by considering a cluster of only five atoms.

It would be of interest to look for a similar effect in three-dimensional systems. An experimental manifestation of this effect would be a great difference in sensitivity of the band-edge states to substitutional impurities or interstitial impurities.

The final general feature of the results is the structure to be observed below the lowest band edge, i.e., at $E \cong 3$. Here the vacancies introduce

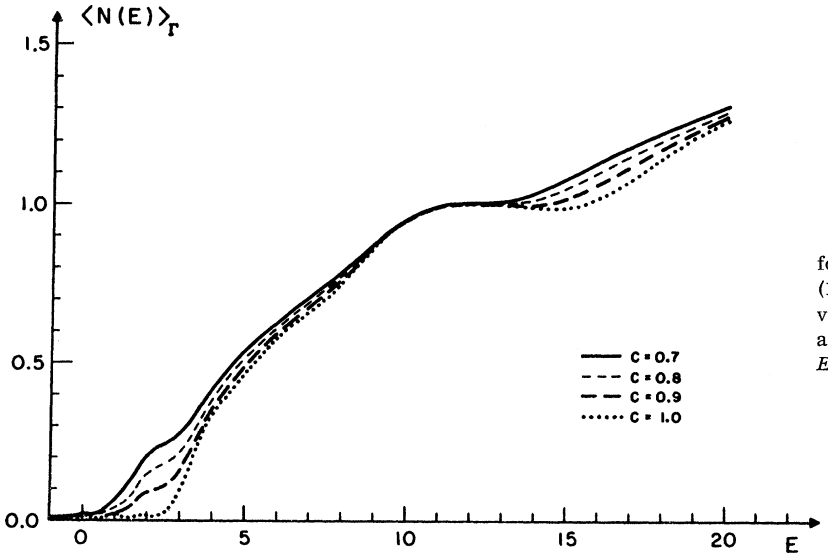

FIG. 5. Echo series calculations for disordered systems. In these curves $(1 - c)$ represents the fraction of vacant sites. The other parameters are the same as in Fig. 4. $N(E)$ and E are in dimensionless units.

slight bumps into the curve of $\langle N(E)\rangle$. By plotting the heights of these bumps and comparing their positions with obvious calculations, we ascribe them to "bound states" in the vacancies. The higher energy bump is approximately linear in c (the vacancy concentration) and has an energy of roughly 2.5. The lower bump, at about $E \cong 1$, is roughly quadratic in c and is conjectured to be the even bound state associated with a pair of nearest-neighbor vacancies.

ACKNOWLEDGMENTS

We are very grateful to Professor J. S. Langer for interesting and valuable comments. The help of the Computer Center of the University of Pittsburgh, where the numerical calculations were performed, is gratefully acknowledged.

APPENDIX: ANALYTIC PROPERTIES OF THE DENSITY OF STATES

The dispersion relation for any one-dimensional lattice (with period b) is implicitly given by an equation

$$\cos qb = \mu(Eq) \,, \tag{A1}$$

where the function $\mu(E)$ is defined and discussed in a paper of Kohn.[16] We follow the notations of that paper, using its formula (2.9) as the definition of $\mu(E)$ so that we need not assume symmetry of the potential about $x = 0$.

The function $\mu(z)$ is an entire function of z. It is real for real energies and the *only* zeros of its derivative $\mu'(z)$ occur for real energies E_n. As z becomes large, $\mu(z)$ approaches $\cos(bz^{1/2})$. These properties are all established in Kohn's paper.[16] The theorem on the zeros of $\mu'(z)$ is decisive in the sequel; it is, in fact, a special case of a well-known theorem of Laguerre, as $\mu(z)$ is a function of genus zero (see Boas[17] for the definition of genus and a proof of Laguerre's theorem).

Now, for real energies in the allowed bands, we have $\mu^2 < 1$, and the density of states per unit length is given by

$$\rho(E) = \frac{1}{\pi}\frac{dq}{dE} = +\frac{1}{\pi b}\left|\frac{\mu'(E)}{[1-\mu^2(E)]^{1/2}}\right| \,.$$

The question is to what extent one obtains the trace of $G(z)$ by merely inserting z for E in this formula. Consider the function

$$g(z) \equiv -\frac{1}{\pi b}\,\frac{\mu'(z)}{[1-\mu^2(z)]^{1/2}} \,. \tag{A2}$$

Because μ is entire, this function $g(z)$ has singularities only at the zeros of the square root, i.e., only at $\mu = \pm 1$.

In the last part of this Appendix, we prove that $\mu = \pm 1$ *only* for real energies (in fact, at the band edges). Temporarily accepting that, and joining these singularities of $g(z)$ by branch lines along the allowed bands, we obtain the complete specification of the first-sheet values of $g(z)$ by the additional requirement that the square root in (A2) be negative imaginary for real z approaching minus infinity. Then we claim that for real energies *in* the allowed bands,

$$\rho(E) = \lim g(E + i\eta) \qquad \text{as } \eta \to 0^+ \,.$$

To prove this, the reader must follow the changes in sign of all the quantities as we move from band to band, starting with the leftmost.

Notice that the second-sheet values of $g(z)$ are simply

$$g_{\mathrm{II}}(z) = -g_{\mathrm{I}}(z) \,, \tag{A3}$$

and so the density of states is completely analytic on *both* sheets. This is, we think, rather interesting and surprising.

Now consider some arbitrary complex z on the first sheet. If C is a small contour surrounding z in the counterclockwise sense, we certainly have

$$g(z) = \frac{1}{2\pi i}\int_C \frac{g(\xi)\,d\xi}{\xi - z} \,.$$

Deform the contour C to one which encircles the allowed bands and is completed by a large circle at infinity. The deformation is only permitted if the integrand is analytic, and this is only true because $\mu = \pm 1$ has no solutions for complex z, which we prove below.

Using the known limiting form of $\mu(z)$ for large z, we conclude that $g(\xi) \to 1/2\pi\sqrt{\xi}$ (i.e., the kinetic energy ultimately dominates the potential energy), and therefore, the large circle does not contribute. Using the Schwarz reflection principle, we have

$$g(z) = \sum_{\text{bands}} \frac{1}{\pi i}\int_{\text{bands}} \frac{\rho(E)\,dE}{E - z} \,,$$

and this integral is simply related to the trace per unit length of $G(z)$, so that we have established

$$\mathrm{Tr}G(z) = -i\pi g(z) \,. \tag{A4}$$

Since $\mu(z)$ is assumed known, this completes the calculation of $\mathrm{Tr}G(z)$.

Now we must show why $\mu = \pm 1$ can only occur for real z, as this property played a decisive role in establishing (A4). Consider the "real lines" of $\mu(z)$ defined by the equation

$$\mathrm{Im}\,\mu(z) \equiv 0 \,. \tag{A5}$$

Along such a line, the imaginary part of $\mu(z)$ is constant (zero) and therefore the imaginary part of the directional derivation of $\mu(z)$, taken in the direction of the line's tangent, is also zero. Hence, the real part of that directional derivative must be nonzero in order to avoid a vanishing of $\mu'(z)$. Thus, the real part of $\mu(z)$ is *monotone* along a real line of $\mu(z)$.

No two such real lines can intersect for complex z. For that would lead to a vanishing of $\mu'(z)$, as can be seen by examining the Taylor's series about the putative intersection point.

A real line cannot form a closed loop in, say, the upper half-plane. For the real part cannot be monotone around a closed loop without a discontinuity [i.e., a nonanalyticity of $\mu(z)$].

Thus, each real line of $\mu(z)$ must terminate, either at infinity or on the real axis. If we examine the points of attachment (E_n) of the real lines to the real axis, we see that they are zeros of μ'. Again examining the Taylor's series about these points, we can classify them into (a) a group which have $\mu(E_n) > 1$, for which the real part is monotone *increasing* as the line leaves the real axis, and (b) a group which have $\mu(E_n) < 1$, for which the real part is monotone decreasing as the line leaves the real axis. These types alternate regularly. Since they cannot cross or join, they must persist out to infinity, where they are reflected in the asymptotic from of $\mu(z)$.

Since these are the only real lines of $\mu(z)$, and since $\mu = \pm 1$ is never satisfied for complex z on any of them, we conclude that $\mu = \pm 1$ never can occur for complex energy.

---

*Work supported in part by the Air Force Office of Scientific Research under Contract No. AFOSR-96-1678 and by the National Science Foundation under Contract No. GU-3184.

†On leave from the Technische Hochschule, Munich, Germany.

[1]M. Lax, Rev. Mod. Phys. 23, 287 (1951).

[2]D. Edwards and J. L. Beeby, Proc. Roy. Soc. (London) A274, 395 (1963); J. L. Beeby, Phys. Rev. 135, A130 (1964); J. L. Beeby, Proc. Roy. Soc. (London) A302, 113 (1967).

[3]P. W. Anderson and W. MacMillan, in *Theory of Magnetism in Transition Metals*, *Course* 37 (Academic, New York, 1967).

[4]C. Kittel, *Quantum Theory of Solids* (Wiley, New York, 1963).

[5]J. Friedel, Phil. Mag. 43, 153 (1952).

[6]J. S. Langer (personal communication).

[7]J. S. Langer, J. Math. Phys. 2, 584 (1966).

[8]J. L. Beeby, in *Lectures on the Many-Body Problem*, edited by E. R. Caianiello (Academic, New York, 1964), Vol. II.

[9]P. Soven, Phys. Rev. 156, 809 (1967).

[10]B. Velický, S. Kirkpatrick, and H. Ehrenreich, Phys. Rev. 175, 747 (1968).

[11]A. H. Wilson, *Theory of Metals* (Cambridge U. P., Cambridge, England, 1953).

[12]J. des Cloizeaux, Phys. Rev. 139, A1531 (1965).

[13]C. Gray and D. Taylor, Phys. Rev. 182, 235 (1969).

[14]W. Kohn and W. Butler (unpublished); W. Butler, thesis, University of California, 1969 (unpublished).

[15]R. More (unpublished).

[16]W. Kohn, Phys. Rev. 115, 809 (1959).

[17]R. P. Boas, *Entire Functions* (Academic, New York, 1954).